

THERMAL TREATMENT SYNTHESIS AND CHARACTERIZATION OF NANOSIZED NICKEL CHROMITE SPINELS.

Syuhada Abu Bakar*, Noorhanim Ahad and Elias Bin Saion

*Department of Physics, Putra University, Malaysia (UPM),
43400 Serdang, Selangor, Malaysia*

**Corresponding author: sab_88star@yahoo.com*

ABSTRACT

The simple preparation of fine-particle nickel chromite (NiCr_2O_4) nanoparticles have been prepared from an aqueous solution containing nickel (II) nitrate, chromium (III) nitrate, polyvinyl pyrrolidone (PVP) as a capping agent and deionized water as a solvent. The mixtures were thermally treated at various temperatures from 450°C to 600°C which the stability of the particles was achieved when the calcination occurred. The synthesized powders were characterized by X-ray diffraction (XRD), Fourier transform infrared spectroscopy (FT-IR), transmission electron microscopy (TEM) and electron spin resonance (ESR). The crystallization of NiCr_2O_4 was completed at 600°C , as publicized by the absence of organic absorption band in FT-IR spectra. XRD results for the calcined samples of the NiCr_2O_4 nanoparticles at different temperatures show the reflection planes of (220), (311), (400), (511) and (440). The main peak was centered at $2\theta = 35.86^\circ$ and corresponds to a crystal plane with Miller indices of (311), which confirm the presence of single-phase NiCr_2O_4 with a face-centered cubic (FCC) spinel NiCr_2O_4 . The magnetic property of NiCr_2O_4 was characterized by ESR where the values of linewidth, ΔH_{pp} and g-factor were increase while the values of magnetic resonance field, H_r , were decreased as calcination temperature increased. The morphology of nanoparticles study by TEM revealed that the size of nickel chromite was estimated in the range around 6 nm to 17 nm.

Keywords: nickel chromite; thermal treatment;

INTRODUCTION

Transition metal chromites possessing spinel structure (an important class of mixed-metal-oxide) with formula of MCr_2O_4 or $\text{MO} \cdot \text{Cr}_2\text{O}_3$ (M= Co, Ni, Zn, Ca or others) can be described as cubic, closely-packed arrangement of oxygen atoms, and M^{2+} and Cr^{3+} ions can occupy either tetrahedral (A) or octahedral (B) sites [1]. This means that the crystal structure consists of either magnetic or nonmagnetic transition metal atoms occupying all of the tetrahedral $8(a)$ sites or magnetic chromium atom occupying all of the octahedral $16(d)$ sites [2]. Such material have widespread use and attracted the attention of some investigators as good catalysts for some industrial reactions for examples NiCr_2O_4 and ZnCr_2O_4 [3], refractory; CaCr_2O_4 and MgCr_2O_4 [4-6], pigments and glazes; CoCr_2O_4 [7].

The preparation of metal chromites nanocrystals through different routes has become a crucial part of research and development in order to achieve materials of the desired physical and chemical properties. More than a few new processing techniques have emerged because some other method for the synthesis of chromite spinel requires a long processing time and high temperature furnace. The most widely used method for the synthesis of chromite spinel involves solid-state reaction metal oxide at high temperature which the unavoidable sintering cause by the high temperature calcination leads to materials with small surface area. Besides, solid-state reaction requires the long-range diffusion of metal ions, which may result in inhomogeneity, larger and nonuniform grains (micron-sized) also poor control of stoichiometry [8][9].

Recently, novel routes were explored to obtain new technique for producing chromite spinel for example wet chemicals route. This type of route has been used for the synthesis of homogenous, sinterable chromite powder with large surface area. By means of microemulsion [10], coprecipitation [11], sol-gel [12], citrate-nitrate gel combustion [13], sol-spray process [14][15], polymeric gel [16] and hydrothermal process [17][18] are some of examples the powder are synthesized in liquid system of wet chemical process. Thermal treatment processes suggest the advantages of low cost production, simple, relatively low reaction temperature, an environmentally friendly alternative and lack of by-product effluents. Moreover, this method contains no other chemicals added to the mixture solution [19]. The mean of this present work was to develop a low temperature thermal treatment route to synthesis nanosized nickel chromite spinels. The textural and morphological characteristic of the prepared nickel chromite nanocrystals were studied with various techniques to validate the influence of calcination temperature on the crystallization, morphology and particle size distribution of the nanocrystals as well as to explore other parameter of interest.

MATERIALS AND METHODS

Nickel chromites used in this experiment were prepared by the thermal treatment method followed by calcinations process. Nickel nitrate and chromium nitrate were used as precursors; polyvinyl pyrrolidone (PVP) was used as a capping agent to reduce agglomeration of the particles. Since, nitrates are the most water soluble of all salts, deionized water was used as the solvent.

Nickel nitrate $\text{Ni}(\text{NO}_2)_3 \cdot 6\text{H}_2\text{O}$ and chromium nitrate, $\text{Cr}(\text{NO}_3)_3 \cdot 9\text{H}_2\text{O}$, were purchased from Acros Organics with purities exceeding 99% while PVP was purchased from Sigma Aldrich (MW = 10000). All chemicals were of analytical reagent grade and were used without further purification. An aqueous solution of PVP was prepared by dissolving 3 gram of polymer in 100 ml of deionized water at 80°C, before it was added into 0.2 mmol of chromium nitrate and 0.1 mmol of nickel nitrate (Cr:Ni = 2:1). The solution was constantly stirred for about 2 hours using magnetic stirrer to make it homogenous. After 2 hours period, a colourless, transparent solution was obtained. A solution was poured into a glass Petri dish and heated at 110°C in an oven for 24 hours

to evaporate water. The brown dried solid chromites that remained were crushed and ground for about 3 hours in a mortar to form a fine powder. The calcinations of the powder were conducted at 450°C, 500°C and 600°C for 4 hours to decompose the organic compounds and crystallize the nanoparticles.

RESULTS AND DISCUSSIONS

The FT-IR spectra analysis with wave numbers of 280 to 4000 cm^{-1} for dried 110°C and calcined samples at 450°C, 500°C and 600°C illustrated in Figure 1. The spectra shows that the absorption bands of Ni-O and Cr-O bonds appeared at wave number of 594 and 478 cm^{-1} respectively, at 600°C for pure spinel NiCr_2O_4 . These bonds provide evidence of the formation of the metal ions-oxygen in tetrahedral and octahedral sites in the spinel structure. The absence of the peaks in the range of 1000-1300 cm^{-1} and 2000-3000 cm^{-1} in the calcined sample at 600°C confirmed that the O-H mode, C-O mode and C=H stretching-mode of organic sources are removed.

Figure 2 shows the XRD pattern for NiCr_2O_4 dried at 110°C and calcined samples at 450°C, 500°C and 600°C. The sharp and broad peaks appearing in the diffractogram confirm the formation of fine nanocrystalline, single-phase and an ordered NiCr_2O_4 phase with a spinel structure along with Cr_2O_3 . The calcined samples of the NiCr_2O_4 nanoparticles at different temperatures of 450°C, 500°C and 600°C for 4 hours show the reflection planes of (220), (311), (400), (511) and (440) respectively. The main peak was centered at $2\theta = 35.86^\circ$ and corresponds to a crystal plane with Miller indices of (311), which confirm the presence of single-phase NiCr_2O_4 with a face-centered cubic (FCC) spinel NiCr_2O_4 [20].

The wide peak for samples dried at 110°C does not have sharp diffraction pattern and still amorphous. As calcination temperature increase to 500°C and 600°C leads to a considerable increase in peak intensity. Meanwhile, the widths of the diffraction peaks become narrower with the increase of calcination temperature, indicate the size of the particles increase. The average particle size of NiCr_2O_4 nanoparticles was determined from full width at half maximum (FWHM) of the XRD patterns using well-known Scherer formula:

$$D = 0.9\lambda / \beta \cos \theta$$

where D is the crystallite size (nm), β is the full width of the diffraction line at half the maximum intensity measured in radians, λ is the x-ray wavelength of Cu $\kappa\alpha = 0.154$ nm and θ is the Bragg angle. The crystallite sizes estimated using the Scherer formula were found to increase with calcination temperature, from about 9.19 nm at 450°C to 18.36 nm at 600°C.

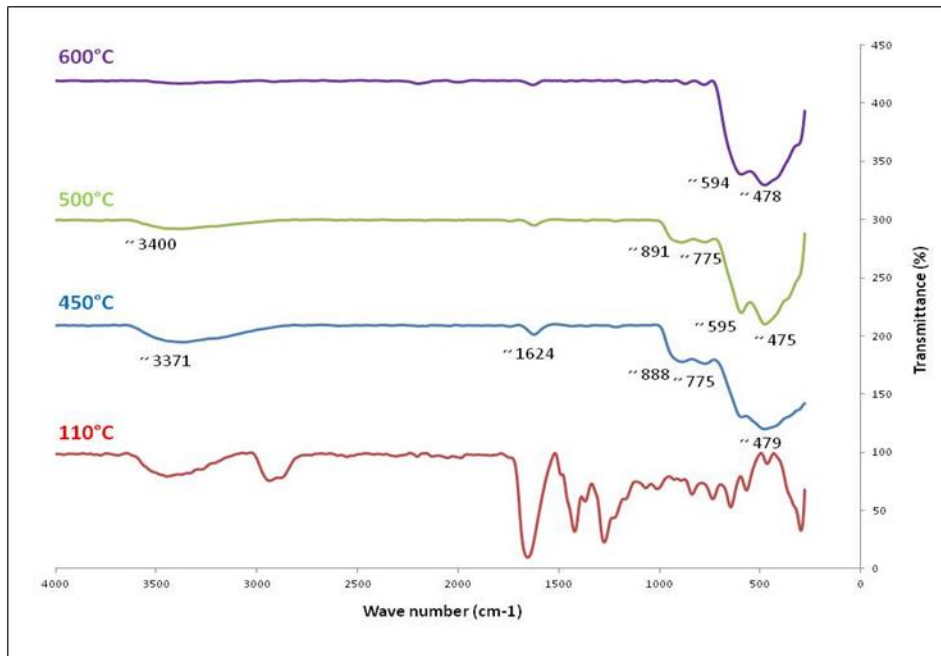


Figure1: FT-IR spectra of NiCr₂O₄ calcined at difference temperatures

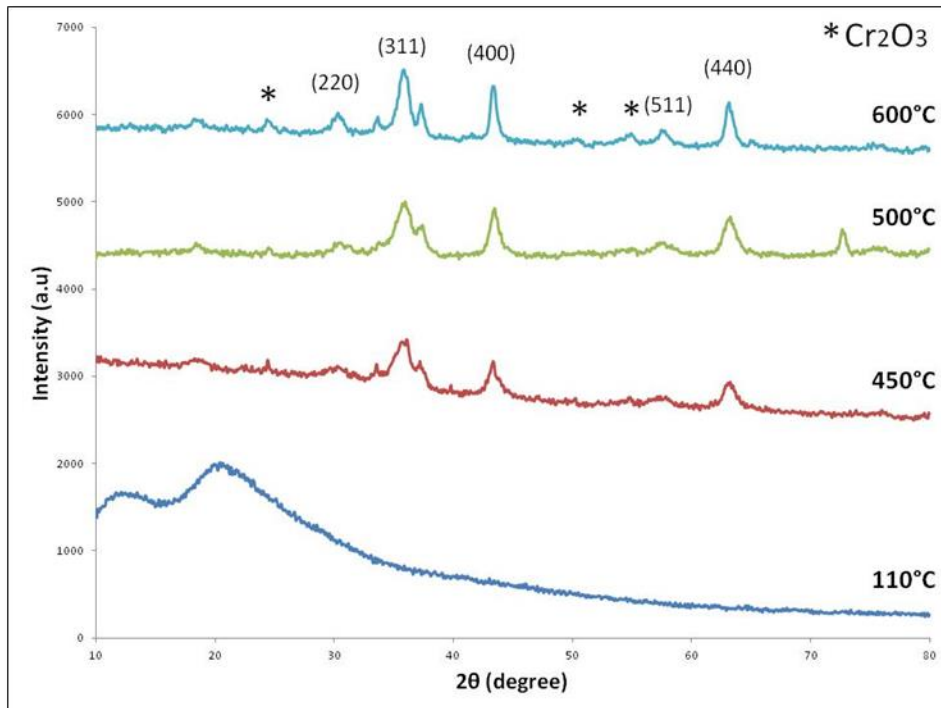


Figure 2: XRD patterns of NiCr₂O₄ calcined at difference temperatures

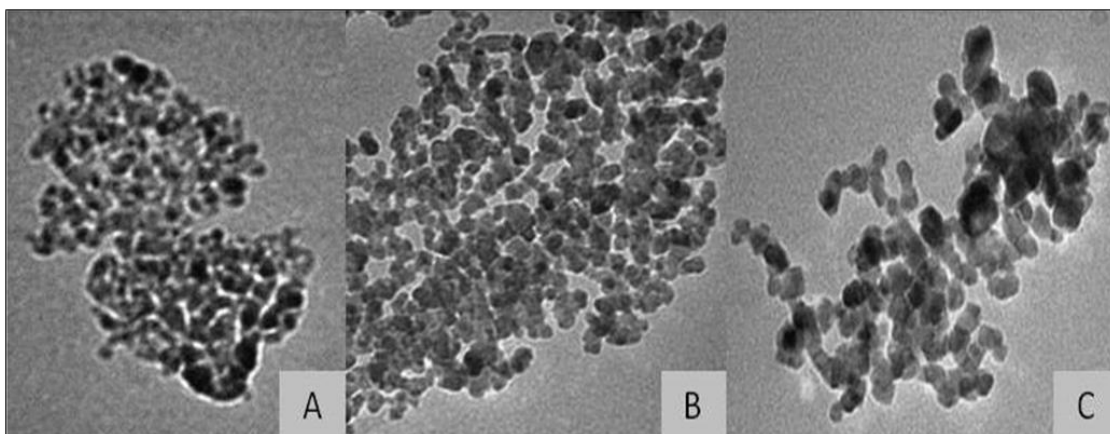


Figure 3: TEM images of nickel chromite calcined at (A) 450°C, (B) 500°C and (C) 600°C in a range of 100 nm

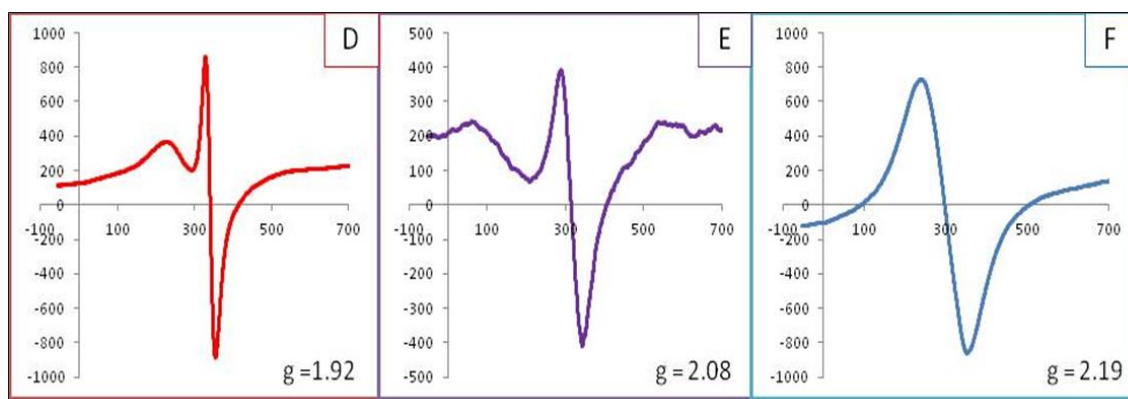


Figure 4: ESR spectra of nickel chromite calcined at (D) 450°C, (E) 500°C and (F) 600°C

Figure 3 shows the TEM images and particle size distribution of NiCr_2O_4 powder calcined at three different temperatures. The results indicate that the samples prepared by thermal treatment method are uniform in morphology and particle size distribution. The smallest size obtained in this work was 6 nm at 450°C and reached 17 nm at the calcination temperature of 600°C. This suggests that the several neighboring particles fuse together to increase particle sizes by melting their surfaces when the calcination temperature increases.

The ESR spectra of the calcined samples are shown in Figure 4. All spectra exhibited broad and symmetrical signals. Peak-to-peak line width (ΔH_{PP}), g-factor and resonant magnetic field (H_r) are three parameters that characterize the magnetic properties. From Table 1, it is obvious that the values of ΔH_{PP} increase from 25.79 to 124.45 Oe and the g-factor also increase from 1.9 to 2.1 when the calcination temperature and particle size increased. In chromites, variations of ΔH_{PP} and g-factor can be due to dipole-dipole

interactions and super-exchange interaction. These suggest that microscopy magnetic interactions increase as particle size increases. According to the equation $g = hv/\beta H$, the resonant magnetic field (H_r), decrease when ΔH_{pp} and g-factor increased. The values of H_r decreased from 340.97 to 289.88 Oe as the calcination temperature increased. The addition of Cr^{3+} ions at 600°C in A site cause an increase in the super-exchange interaction, contributing to a decrease in the resonant magnetic field.

Table 1: The values of magnetic resonance field, g-factor and linewidth of $NiCr_2O_4$ calcined at different temperatures

Samples	Calcination temperature (°C)	Magnetic resonance field H_r (Oe)	Geomagnetic ratio (g-factor)	Linewidth ΔH_{pp} (Oe)
$NiCr_2O_4$	450	340.97	1.92	25.79
$NiCr_2O_4$	500	314.50	2.08	53.33
$NiCr_2O_4$	600	289.88	2.19	124.45

CONCLUSION

The spinel nickel chromite, $NiCr_2O_4$, nanocrystals were successfully synthesized by thermal treatment method utilizing only nickel nitrate and chromium nitrate as precursors, deionized water as a solvent and PVP as a capping agent. They were thermally treated at various temperatures to stabilize the particles from 450°C to 600°C, at which calcination occurred, thereby preventing their agglomeration, stabilizing the particles, controlling the growth of the nanoparticles and creating a uniform distribution of the particles sizes. Particles sizes of 6 nm to 17 nm were obtained with calcination temperatures between 450°C and 600°C as confirmed by XRD and TEM analyses.

The organic compounds and nitrate ions were completely removed at the calcination temperature of 600°C. The magnetic studies showed that the values of ΔH_{pp} and g-factor of the $NiCr_2O_4$ increased meanwhile the values of H_r decreased as the calcination temperature increased, confirmed that these $NiCr_2O_4$ nanoparticles have a magnetic behavior. Finally, FT-IR spectra and TEM images are used to investigate the process in the absence of PVP and other organic compound that pollute the crystal lattice during preparation as well as to study the allocation size of $NiCr_2O_4$. These uncomplicated, relatively low reaction temperatures, cost-effective and environmentally friendly method that produces no by-product effluents [20] can be used to fabricate pure crystalline spinel $NiCr_2O_4$ nanoparticles with a small size about 6-17 nm. Besides, this simple method may be extended to fabricate other spinel chromite nanoparticles of interest in sciences and technology.

ACKNOWLEDGEMENT

The authors would like to thank the laboratory facilities provided by the Department of Physics, Faculty of Science, Universiti Putra Malaysia.

REFERENCES

- [1]. B. Aslibeiki, P. Kameli, H. Salamati, M. Eshraghi, T. Tahmasebi, *J. Magn. Magn. Mater* 322 (2010) 29292934.
- [2]. Marinkovi Stanojevi Z.V., Romevi N., Stajanovi B.J., *Eur.Ceram. Soc.* **27** (2007) 903-907
- [3]. R.J. Klingher and J.N. Rathke, *J. Am. Chem. Soc.* **106** (24) (1984) 7650
- [4]. W.T. Bakker, S.Greenberg, M. Trondt, and U. Gerhardus, *Am. Ceram. Soc. Bull*, **63** (7) (1986) 870-876
- [5]. S.M. Wiederhorn and R.F. Krause, Jr., *J.Am.Ceram. Soc.* **67** (7) (1988) 1202
- [6]. J. Zborowski, W. Kronert, F. Nadachowski, and G. Dhupia, “ Microstructural Changes of CaO-Cr2O3 Refractory under Slag Attack”, p.2415 in High Tech Ceramic, Edited by P.Vincenzini, Elsevier Science, Amsterdam, Netherland, 1987.
- [7]. “Industrial Applications of Cobalt Compounds”, p.306 in Ullmann’s Encyclopedia of Industrial Chemistry, vol.A7, Edited by W.Gerhantz, Weinheim, New York, 1988.
- [8]. Fern´andez Colinas, J. M.; Otero Are´an, C. *J. Solid State Chem.* **109** (1994) 43-46
- [9]. Durrani, S. K.; Akhtar, J.; Hussain, M. A.; Arif, M.; Ahmad, M. *Mat. Chem. Phys.* **100** (2006) 324-328
- [10]. Uskokovi, V.; Drogenik, M. *Surf. Rev. Lett.* **12** (2005) 239-277
- [11]. Patil, K. C.; Hegde, M. S.; Rattan, T.; Aruna, S. T. (Eds.) *Chemistry of Nanocrystalline Oxide Materials:Combustion Synthesis, Properties and Applications*, World Scientific Publishing Company, Singapore, 2008.
- [12]. Yazdanbakhsh, M.; Khosravi, I.; Goharshadi, E. K.; Youssefi, A. *J. Hazard. Mater.* 184 (2010) 684-689
- [13]. Durrani, S. K.; Hussain, N.; Saeed, K.; Ahmad, M.; Siddique, M.; Ahmad, N.; Qazi, N. K. *The Nucleus* **47** (2010) 17-23
- [14]. Durrani, S. K.; Qureshi, A. H.; Qayyum, S.; Arif, M. *J. Therm. Anal. Calorim.* **95** (2009) 87-91.
- [15]. Durrani, S. K.; Saeed, K.; Qureshi, A. H.; Ahmad, M.; Arif, M.; Hussain, N.; Mohammad, T. *J. Therm. Anal. Calorim.* **104** (2011) 645-651.
- [16]. Gama, L.; Ribeiro, M. A.; Barros, B. S.; Kiminami, R. H. A.; Weber, I. T.; Costa, A. C. F. M. *J. Alloy. Comp.* **483** (2009) 453-455.
- [17]. Zawadzki, M. *Solid State Sci.*, **8** (2006) 14-18
- [18]. Durrani, S. K.; Khan, Y.; Ahmed, N.; Ahmad, M.; Hussain, M. A. *J. Iran. Chem. Soc* **8** (2011) 562-569

- [19]. M.Goodarz Naseri, E. Bin Saion, H. Abbastabar Ahangar, M. Hashim, A.H. Shaari, *Powder Technology* **212** (2011) 80-88
- [20]. S.K. Durrani, S.Z. Hussain, K. Saeed, Y. Khan, M. Arif, N. Ahmed, *Turk J Chem* **36** (2012), 111-120